Taylor & Francis
Taylor & Francis Group

RESEARCH PAPER

Short-term *ex-vivo* exposure to hydrogen sulfide enhances murine hematopoietic stem and progenitor cell migration, homing, and proliferation

Anoushka Khanna ⬤[a,b], Namita Indracanti[a], Rina Chakrabarti[b], and Prem Kumar Indraganti ⬤[a]

aDrug Repurposing and Translational Research Lab, Institute of Nuclear Medicine and Allied Sciences, Defence Research and Development Organization, Delhi, India; bAqua Research Laboratory, Department of Zoology, University of Delhi, Delhi, India

ABSTRACT

For successful transplantation of Hematopoietic Stem cells (HSCs), it is quite necessary that efficient homing, engraftment and retention of HSC self-renewal capacity takes place, which is often restricted due to inadequate number of adult HSCs. Here, we report that short-term *ex-vivo* treatment of mouse bone marrow mononuclear cells (BMMNCs) to Sodium Hydrogen Sulfide (NaHS, hydrogen sulfide-H_2S donor) can be used as a possible strategy to overcome such hurdle. H_2S increases the expression of CXCR4 on HSPCs, enhancing their migration toward SDF-1α in-vitro and thus homing to BM niche. . Additionally, *in-vitro* studies revealed that H_2S has a role in activating mitochondria, thus, pushing quiescent HSCs into division. These results suggest a readily available and cost-effective method to facilitate efficient HSC transplantation.

Introduction

Hematopoietic Stem Cell (HSC)'s ability to self-renew and also to differentiate into hematopoietic lineages, render them indispensable for hematopoietic stem cell transplantation (HSCT). Umbilical cord blood is a rich source of HSCs and is of great use to treat hematological disorders (malignant and non-malignant) where HSCT is inevitable [1]. The inadequate number of HSCs per unit cord blood (CB) is a major hindrance to their use. One way to overcome this, is to enhance the homing efficiency of transplanted HSCs which can subsequently repopulate successfully, thus showing improved engraftment efficacy, even with limited numbers of HSCs, thereby circumventing the need for *ex-vivo* HSC expansion [2].

Several expensive molecules and strategies have been identified for *ex-vivo* manipulation of HSC grafts which can increase the efficiency of transplantation and provide successful outcomes [2]. One such strategy is hypoxia preconditioning of bone marrow mesenchymal stem cells by dimethyloxalylglycine (DMOG) which is hypoxia inducible factor 1α (HIF-1α) prolyl hydroxylase enzyme inhibitor, in order to promote HSC survival after transplantation [3,4]. Transition from hypoxic bone marrow niches to non-physiological ambient air during HSC collection leads to ROS production and opening of mitochondrial permeability transition pore

(MPTP), causing poor HSC survival and loss of their long-term repopulating potential [5–7]. Isolation of HSCs in the presence of MPTP inhibitor Cyclosporin A has been reported to recover long-term HSCs, provides better survival and enhanced transplantation efficiency [5]. In addition to it, modulation of calcium-sensing receptor (CaR) by treating HSCs with CaR agonist Cinacalcet has been reported to enhance HSC homing, lodgment, and engraftment [8,9]. Apart from this, ex-vivo exposure of HSCs to prostaglandin E_2 (PGE$_2$) has also been implicated to facilitate efficient transplantation by increasing HSC frequency, homing and full multilineage reconstitution [10].

H_2S is accepted to be an endogenous gasotransmitter, which regulates various signaling cascades and cell homeostasis in mammalian cells, whose abnormal levels have been linked to various human diseases [11–13]. H_2S is produced in mammals via L-cysteine catalyzed by enzymes cystathionine β-synthase (CBS), cystathionine γ-lyase (CSE) and 3-mercaptosulfurtransferase, of which CBS is predominantly expressed in brain, CSE in smooth muscles and latter in neurons, vascular endothelium, and the retina apart from other organs [14,15]. Recent studies have demonstrated the role of H_2S production by bone marrow mesenchymal stem cells (BMMSCs) to maintain their self-renewal and bone homeostasis via regulation of Ca^{2+} channel sulfhydration. They further reported that H_2

CONTACT Prem Kumar Indraganti ✉ prem@inmas.drdo.in ⬤ Drug Repurposing and Translational Research Lab, Institute of Nuclear Medicine and Allied Sciences, Defence Research and Development Organization, Delhi 110054, India

S deficiency leads to defects in osteogenic differentiation, which is attributed to abnormal intracellular calcium levels, thus suggesting that H_2S has a role in regulating BMMSCs and the restoration of H_2S levels by exogenous donors may be useful for the treatment of related disorders [16]. There is an increasing body of evidence that the impact of H_2S in biological functioning is driven by higher influx of calcium that can be attributed to modulation of calcium channels (L-Type, T-Type, transient receptor potential (TRP) channels) via protein S-sulfhydration and polysulfide reactions [17–19].

In this study, NaHS was used as an H_2S donor and it is reported that H_2S caused a significant increase in intracellular calcium via influx through plasma membrane (in the presence of external calcium) and release from intracellular stores upon short term ex-vivo exposure of BMMNCs to NaHS. A significant dose-dependent upregulation of CXCR4 (chemokine receptor) in NaHS treated BMMNCs was also demonstrated, which can be linked to rise in intracellular calcium, since it is already well established that external calcium treatment of bone marrow cells displays an increase in both mRNA expression along with surface expression of CXCR4 [20]. Furthermore, pulse exposure of NaHS ex-vivo enhanced the homing and lodgment of HSPCs to BM niche as compared to vehicle control, mediated through elevated CXCR4 expression and chemotaxis toward stromal-derived factor1α (SDF1α). Thus, in this report modulation of CXCR4-SDF1α axis which directs the migration and trafficking of HSPCs from circulation to BM microenvironment is implicated as one of the strategies to increase homing and transplantation efficiency [21,22]. Apart from this, NaHS pulse exposure also resulted in the activation of mitochondria via slight elevation of MMP, mitochondrial mass and superoxide thus exhibiting enhanced cell proliferation and cell differentiation, perhaps, indicating the role of H_2S in the activation of calcium mitochondrial pathway which drives quiescent HSPCs into division [23]. Overall, it is concluded that NaHS is a cost-effective method for achieving successful homing and hence efficient transplantation.

Materials and methods

Animal experiments and irradiation

Inbred male mice (C57BL/6) aged 10–12 weeks (weight: 25 ± 2 g) were used for bone marrow harvests and transplantation while engraftment studies were done in female mice (C57BL/6). Mice were provided with unlimited mouse chow and water *ad libitum*. Animal handling and all animal experiments followed protocols approved by Committee on the Ethics of Animal Experiments, Institute of Nuclear Medicine and Allied Sciences (INMAS), Defense Research and Development Organization (DRDO). The animals were kept in the animal house facility under approved optimum conditions. All efforts were made to minimize the number of animal animals used and the suffering they underwent.

Mice were given total body ionizing radiation using γ-ray irradiator (Bhabatron-II Telecobalt Unit, Pancea Medical Technologies, Bangalore, India) and they were exposed in a group of 4. The animals were exposed to lethal dose of radiation (9 Gy) with the irradiation field size of 35 cm x 35 cm and the animals were partially restrained to avoid shielding during the period of radiation exposure.

Isolation of BMMNCs and hydrogen sulfide pulse-exposure

Whole bone marrow (WBM) cells were flushed out from the cavities of tibia and femur of mice using Iscove's Modified Dulbecco's Media (IMDM, Stem Cell Technologies) supplemented with 10% heat-inactivated Fetal Bovine Serum (HI-FBS, CELLect™ FBS Gold) and 100 U/ml penicillin, and 100 mg/ml streptomycin (SIGMA). Single cell suspension was obtained by passing through a cell strainer (BD Biosciences). For flow cytometric analysis, WBM cells were subjected to RBC lysis (ice cold 1x Ammonium Chloride potassium buffer) and finally the cells were washed and resuspended in IMDM media (+10%FBS). For pulse exposure, Sodium hydrogen sulfide (NaHS) (Sigma) was dissolved in media and used as a donor of H_2S. Bone marrow mononuclear cells (BMMNCs) ($5x10^6$) were resuspended in 2 ml of media and incubated with 300 μM NaHS for 30 min (with intermittent tapping) in a CO_2 incubator at 37°C (5%CO_2, 95% humidity). In case of Bone marrow transplantation, WBM cells (without RBC lysis) were treated with NaHS similarly as mentioned above. After incubation, the cells were washed in PBS+2% FBS twice before further use. Untreated cells (Control) were also processed in the same way.

Lineage depletion and flow cytometry

For flow cytometry experiments, lineage depletion of H_2S-treated and untreated cells was carried out using the mouse lineage cell depletion kit following the manufacturer's protocol (Miltenyi Biotec). BMMNCs were incubated with biotin-conjugated antibodies against Lineage markers (CD5, Mac-1, CD45R/B220, Ter-119,

and Gr-1) and thereafter they were incubated with anti-biotin microbeads for 20 mins on ice. Cells were washed with PBS and magnetic separation was performed with an LD MACS column (Miltenyi Biotec) to obtain the lin ^{neg} fraction which was washed and resuspended in binding buffer (PBS+2% Bovine serum albumin). The cell number was volumetrically determined using flow cytometer [24] and further to analyze different subsets of hematopoietic stem and progenitor cells (HSPCs), they were pre-incubated with anti-CD16/32 antibody (0.5 μL/10^6 cells; Biolegend, CA, USA) to block the Fcγ receptors and then stained with anti-Sca1-PE (2 μL/10^6 cells; BD biosciences), c-Kit-APC (2 μL/10^6 cells; BD biosciences) and anti-mouse CD34-PerCp (2 μL/10^6 cells; Biolegend) at room temperature, in the dark for 30 min. Following incubation, the cells were washed and finally the frequencies of LSK, ST-HSCs and LT-HSCs were analyzed via Flow cytometry using BD Accuri C6 software [25,26]. For evaluating CXCR4 expression, BMMNCs were treated with Vehicle/NaHS/BAPTA-AM (Calcium chelator), incubated for 30 min at 37°C, washed and cultured in IMDM+10% HI-FBS [supplemented with 2 mM L-glutamine (Himedia) and 100 U/ml penicillin, and 100 mg/ml streptomycin (Sigma)] for 24 h in a CO_2 incubator (37°C, 5% CO_2). After 24 h, the cells were processed in the same way as mentioned above and stained for surface markers along with CXCR4 antibody (anti-mouse CD184-PerCp, 2 μL/10^6 cells; Biolegend), and CXCR4 expression was quantified in different subsets of HSPCs via Flow cytometer.

RNA extraction and CXCR4 gene expression analysis

Total RNA was extracted from NaHS treated, BAPTA-AM treated and untreated BMMNCs after 24 h of culture using RNeasy mini kit (Qiagen) and quantified using Nanodrop (Thermo scientific). A fixed amount of RNA was then reverse-transcribed using cDNA synthesis kit (Biorad) following manufacturer's instruction. cDNA template was diluted 20 times and Quantitative Real-Time PCR was performed using SsoFast EvaGreen Supermix (Biorad) and CFX96 (Biorad) Real-Time PCR system. The sequences of primers used for amplification are as mentioned (Table 1). The reaction was set up under the following conditions: 95°C for 30 s, 50 amplification cycles of 95°C for 5 s, 54°C for 5 s and 72°C for 15 s, followed by a melting-curve step to ensure single product formation. The relative mRNA expression was calculated using Livak method and was normalized to the level in vehicle control, that was set to 1 [27]. For time point studies, cells were treated with

Table 1. Primers used for amplification.

Gene	Primer sequence
CXCR4 [28]	F: 5'-TCTATGTTGGCGTCTGGATCC-3'
	R: 5'- CTTGGAGTGTGACAGCTTGG-3'
β-actin	F: 5' ATAAGAGACAACATTGGCATGGCTT-3'
	R: 5'-TCGCCTTCACCGTTCCAGTT-3'

300 μM of NaHS or vehicle control, washed and cultured and further the expression was determined at different time points (14, 24, and 36 h).

Trans well migration assay

To determine the CXCR4-SDF1α (Stromal Derived Factor 1- alpha) interaction, chemotaxis assay was performed using Costar 24-well Transwell plates (6.5 mm diameter inserts, 8.0 μm PET membrane, Corning, USA). 600 μl of IMDM containing SDF1α (100 ng/ml, Miltenyi Biotec) was poured into the bottom chamber [29]. Lin^{neg} cells either treated with NaHS (300 μM) or with vehicle and were cultured in IMDM+10% HI-FBS for 24 h allowing for the up-regulation of CXCR4 expression. Additionally, 30 m prior to this assay replicate cells were treated with a CXCR4 antagonist, AMD3100 (10 μM) to block the receptor. Thereafter, the cells were washed and resuspended in IMDM+0.5% BSA. The cells were volumetrically enumerated and 100 μl of cell suspension ($2x10^5$ cells) was added to the top chamber of the trans well plate. The plates were then incubated for 4 h at 37°C, 5% CO_2 and 95% humidity. The cells that migrated to the bottom chamber were stained with surface marker antibodies and enumerated by flow cytometry.

Cell viability and apoptosis assay

HEK (Human Embryonic Kidney) cells were seeded at a density of 5×10^3 per well in a 96-well culture plate and kept overnight in the incubator (37°C, 5% CO_2, 95% humidity) for the cells to adhere. Subsequently, the cells were treated with NaHS from a dose range of 100 μM to 1 mM along with vehicle control. After 24 h of treatment, the cells were washed and MTT [3-(4, 5- dimethyl thiazolyl-2)-2,5-diphenyltetrazolium bromide] reagent (1 mg/ml, Himedia) was added to each well and incubated for 4 h under the same conditions. Thereafter, 150 μl of DMSO was added to dissolve the insoluble formazan crystals and the absorbance was read at 570 and 670 nm as a reference. Percentage viability was calculated as specific absorbance of test divided by specific absorbance of control x 100.

BMMNCs were treated with 300 μM of NaHS or with vehicle control, and incubated for 24 h in IMDM +10% HI-FBS (100 U/ml penicillin, and 100 mg/ml streptomycin). Following the incubation, the cells were lineage-depleted, stained for surface markers (LSK) along with AnnexinV-FITC (BD Biosciences) and 7-AAD (BD Biosciences) according to the manufacturer's protocol and the proportion of apoptotic and dead cells were determined flow cytometrically in Lin [neg] and LSK population.

Colony Forming Unit (CFU) assay

BMMNCs were treated with NaHS or vehicle control, washed, and resuspended in IMDM+2% FBS. The cell suspension (30,000 cells/plate) was added to the Methocult methyl cellulose medium (GF M3434, Stem Cell Technologies) in 1:10 ratio and mixed by vortexing. The cell suspension was dispensed using 16-gauge blunt end needle (stem cell technologies) into culture plates and incubated at 37° C, 5% CO_2 and 95% humidity. After 14 days, BFU-E (burst forming unit-erythroid), CFU-GM (colony-forming unit granulocyte, macrophage) and CFU-GEMM (CFU-granulocyte, erythroid, macrophage, megakaryocyte) were scored and the data were expressed as number of CFUs/30,000 input cells [30].

Hematopoietic stem and progenitor cell homing

To evaluate the homing efficiency, host mice were lethally irradiated (10 Gy) using ^{60}Co γ-ray irradiator (Bhabatron-II Teletherapy Unit, Panacea Medical Technologies, Bangalore, India) 24 h before transplantation to deplete the whole bone marrow. WBM cells (3x10^6) from donor mice were treated with NaHS or vehicle as described previously, washed, and resuspended in PBS+2% FBS. The cells were then labeled with 5 μM Carboxyfluorescein diacetate succinimidyl ester (CFSE) for 15 min at 37°C in the dark with intermittent mixing [31]. Thereafter, the labeled cells (CFSE[+]) were thoroughly washed with ice-cold PBS to remove any unbound CFSE from the cell suspension and infused into lethally irradiated hosts via the tail vein to assess the HSPC homing. The host animals were sacrificed 16 h after infusion, BMMNCs isolated, lineage depleted and the Lin [neg] cells were stained with anti-mouse Sca1-PE (2 μL/10^6 cells; BD biosciences), c-Kit-APC (2 μL/10^6 cells; BD biosciences), CD34-PerCp (3.5 μL/10^6 cells, Biolegend) and homing of different subsets of CFSE[+] HSPCs (Lin [neg], LSK, ST-HSC, LT-HSC) was

determined flow cytometrically and the mean fluorescence intensity was noted.

In-vitro cell proliferation and cell cycle analysis

BMMNCs were treated with NaHS or vehicle, washed, and cultured in α-MEM+10% HI-FBS (+2 mM L-Glutamine-HIMEDIA, 100 U/ml penicillin, and 100 mg/ml streptomycin) for 24 h at 37°C (5% CO_2, 95% humidity). For cell cycle analysis, cultured cells were washed, lineage depleted, and stained with surface marker antibodies (c-kit, Sca-1). After that, the cells were fixed in 4% Paraformaldehyde (PFA), permeabilised (with PBS-Tween 20), washed and stained with 7-aminoactinomycin-D (AAD) along with RNase (50 μg/mL) treatment for 15 m on ice. The proportion of Lin [neg] and LSK population in different phases of cell cycle were then analyzed via flow cytometer. For the determination of cell proliferation, BMMNCs were treated similarly, cultured for 24 h, lineage-depleted and stained. Subsequently, Lin [neg] cells were fixed, permeabilised, stained with anti-mouse Ki67-FITC (cell proliferation marker, Miltenyi Biotec) and the proportion of Ki67 positive cells (FITC positive) along with their Mean fluorescence intensity (MFI) was determined flow cytometrically.

Analysis of mitochondrial activity: measurement of mitochondrial membrane potential, mitochondrial mass, superoxide and intracellular calcium

Freshly isolated BMMNCs were treated with NaHS or vehicle, washed and cultured in α-MEM (Stem cell technologies) +10% HI-FBS (supplemented with 2 mM L-glutamine, 100 U/ml penicillin, and 100 mg/ml streptomycin) for 1, 6 and 24 h. After respective time points, the cells were washed, and stained for surface marker antibodies. The mitochondrial membrane potential ($\Delta\Psi_m$), mitochondrial mass and mitochondrial superoxide level were determined using Rhodamine-123 (Rh-123, 2 μM), Mito Tracker Green (30 nM, Molecular Probes) and MitoSOX Red (Mitochondrial Superoxide Indicator; 3 μM, Molecular Probes) respectively, following the manufacturer's protocol. For measuring intracellular calcium, BMMNCs were lineage depleted, stained for surface markers and treated with NaHS or vehicle or Nifedipine (60 μM, Enzo life sciences) in the presence and absence of calcium in PBS. Similar experiment was performed in phenol red-free medium. The cells were simultaneously stained (along with surface marker antibodies) with Fluo-3 AM (3 μM, Thermo Fisher Scientific) and the mean fluorescence intensity was measured after 30 min.

Repopulation of HSCs

BMMNCs were treated with NaHS or with vehicle as previously described, washed, and transplanted into lethally irradiated (9 Gy; Acute dose) mice after 24 h of radiation exposure. After 21 days, peripheral blood was collected and changes in various hematopoietic parameters were evaluated using hematology analyzer (Euro count Plus).

Results

NaHS mediated H_2S release, enhances CXCR4 expression and chemotaxis to SDF-1a

Chemoattraction between chemokine ligand SDF-1α and CXCR4 receptor guides the migration of HSPCs to their niche in both humans and mice. Upregulation of CXCR4 expression on HSPCs is extremely important to find their way to BM and exhibit enhanced homing after transplantation [22]. Hence, in this study, the CXCR4 mRNA expression as well as CXCR4 surface protein expression was evaluated, in-vitro, in NaHS and vehicle-treated cells (Figure 1(a)). qRT-PCR study was performed with different concentrations of NaHS and maximum gene expression was observed when BMMNCs were treated with 300 µM of NaHS (3.4 fold). After this, CXCR4 expression was quantified at various time points (14, 24, and 36 h) using the above concentration of NaHS and BMMNCs revealed an increase in CXCR4 gene expression at all time points of which, 24 h displayed the maximum upregulation in comparison with the vehicle control (Figure 1(b,c)). Additionally, pulse exposure to NaHS also enhanced the surface expression of CXCR4 which was reflected by significant increase (**$p < 0.01$) in mean fluorescence intensity (MFI) in LSK, ST-HSCs, and LT-HSCs population when compared with control (Figure 1(d)). Both CXCR4 mRNA and surface expression were reduced in the presence of BAPTA-AM (intracellular calcium chelator), thus implicating the role of calcium in CXCR4 expression. To further evaluate the chemotaxis between SDF-1α and CXCR4, in-vitro trans-well migration assay was performed. It was observed that significant number of Lineage negative (lin^{neg}) and Lin^{neg}Sca1$^+$c-kit$^+$ (LSK) cells migrated toward 100 ng/ml of SDF-1α (bottom chamber) in both control and treated groups with a significantly increased migration in NaHS treated cells. The frequency of cells migrated, increased up to 2.5-fold, and 1.87-fold in lin^{neg} and LSK population, respectively, in the case of NaHS treated cells as compared to vehicle control (Figure 1(e,f)). Additionally, significant increases in the migration of short-term (ST-HSCs; Lin^{neg}Sca1$^+$c-kit$^+$CD34$^+$ cells) and long-term HSCs (LT-HSCs; Lin^{neg}Sca1$^+$c-kit$^+$CD34$^-$ cells) were also evident (Figure 1(g,h)). The enhanced chemotaxis of HSPCs due to NaHS treatment was significantly blocked by AMD3100, a CXCR4 receptor antagonist [32], which was marked by a reduction of 5.73 and 4.92-fold (Lin^{neg} and LSK, respectively) in comparison with NaHS treated migrated cells, thereby specifically illustrating that HSPCs trafficking and migration is mediated through chemokine receptor CXCR4.

H_2S increases HSPC homing efficacy

The processes of migration and homing are reflection to each other, dependent on the SDF-1α/CXCR4 interplay which is considered essential to direct HSCs and to establish residence in their microenvironment that are prerequisites to subsequent lodging and engraftment [33]. The enhanced migration of NaHS treated cells toward SDF-1α through in-vitro studies have already been reported. To further investigate the potential of NaHS in-vivo, CFSE-labeled NaHS or vehicle-treated BMMNCs were infused into lethally irradiated mice to evaluate the homing of HSCs. Total CFSE$^+$ lin^{neg} homed cells along with homed events within different subsets of BMMNCs were measured flow cytometrically (Figure 2(a)). The results obtained indicate that *ex-vivo* exposure to NaHS led to a significant increase in the number of CFSE$^+$ homed cells with 1.53,1.89,1.32 and 3.5-fold increase in the CFSE$^+$ lin^{neg}, LSK, ST-HSC, and LT-HSC subsets, respectively, as compared to vehicle control (Figure 2(b–d)). Now, it is evident that enhanced homing efficiency is an outcome of CXCR4 upregulation and increased chemotactic interplay between SDF-1α/CXCR4 axis.

H_2S enhances HSPC proliferation and differentiation

Inside the BM niche HSCs reside in quiescent state and become active under stress conditions and initiate hematopoiesis. A correct balance between HSC division and self-renewal is important for their maintenance and efficient hematopoiesis [34]. To assess the differentiation potential of the treated BMMNCs, CFU assay was performed and the colonies were counted on the 14th day. Significant increases in the formation of CFU-GM (vehicle: 34.00 ± 5.033, NaHS: 65.67 ± 8.686) and CFU-GEMM (Vehicle:2.033 ± 0.03333, NaHS: 3.333 ± 0.3333) colonies were detected in NaHS treated cells whereas no significant increase in the number of BFU-E colonies was observed thus, indicating an enhanced differentiation of HSPCs resulting from ex-vivo NaHS exposure (Figure 3(a,b)). Cell proliferation
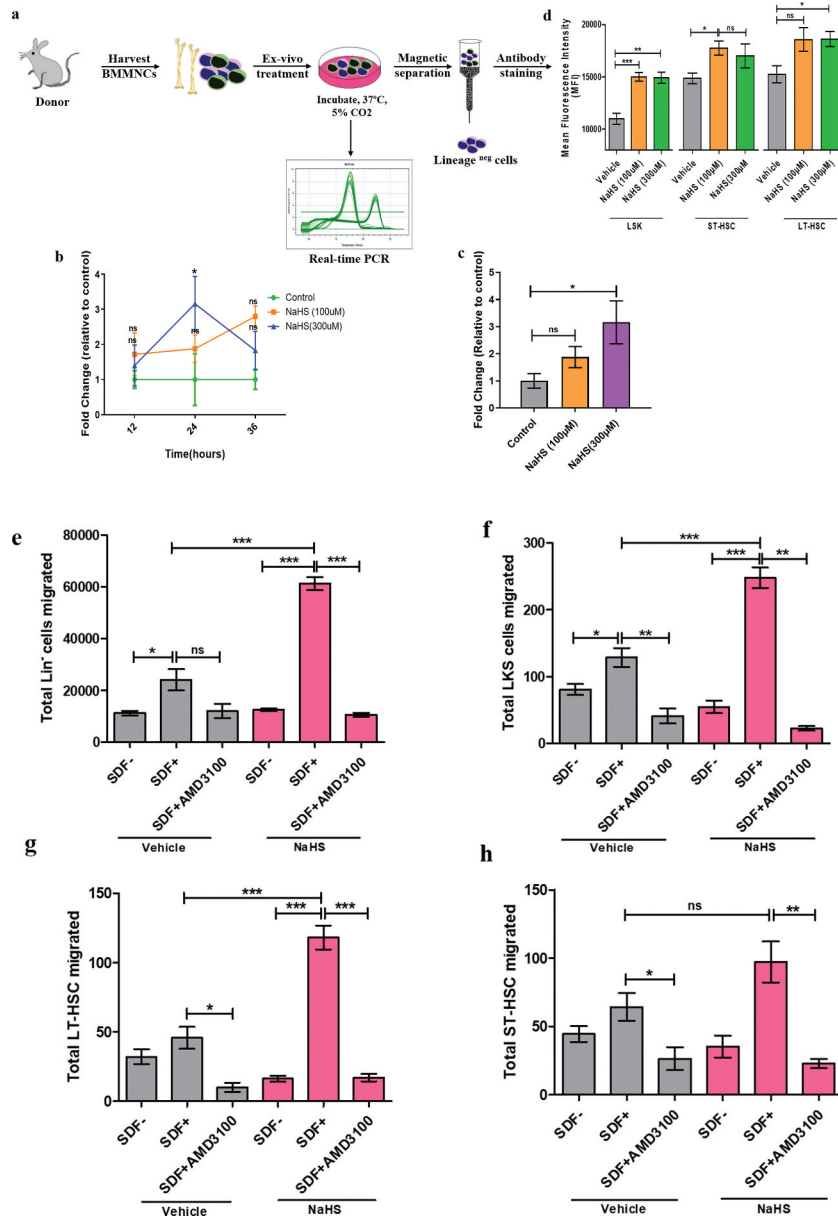
Figure 1. Enhanced CXCR4 receptor expression on NaHS treated BMMNCs and chemotaxis of HSPCs toward SDF-1α. (a) Representative experimental setup for evaluating CXCR4 expression and other parameters. Total BMMNCs were isolated and treated with either vehicle or NaHS for 20 min, washed and cultured in IMDM+10% HI-FBS for 24 h. (b) mRNA amplification plots of CXCR4 receptor on BMMNCs. Relative mRNA expression was calculated using Livak method and β-Actin as a house keeping gene. Time course plot for CXCR4 expression after 12, 24 and 36 h of treatment with vehicle or NaHS to optimize the time point for maximum CXCR4 expression after treatment. (c) Changes in the CXCR4 expression in vehicle/NaHS (100 and 300 μM) treated BMMNCs after 24 h using real time PCR. Data are expressed as mean ± SEM fold change in expression with respect to control (n = 4) and the comparisons were done using one-way ANOVA. Lin^{neg} cells were sorted from freshly isolated BMMNCs, exposed to NaHS/vehicle, washed and cultured in media for 24 h (37ºC, 5%CO_2, 95% humidity). Thereafter, the cells were washed and resuspended in IMDM +0.5%BSA and were allowed to migrate for 4 h. The number of different subsets of HSPCs migrated to the bottom chamber in the presence or absence of SDF-1α were quantified using flow cytometry; (d)Total Lin^{neg} cells migrated (e), Migration of gated LSK population (f), Migration of LT-HSCs (CD34$^-$) and (g) total ST-HSCs (CD34$^+$) migrated. Data are expressed as mean ± SEM total number of cells migrated. (n = 3, ns = non-significant *$p \leq 0.05$, **$p \leq 0.01$ and ***$p \leq 0.001$) and analyzed using one-way ANOVA.

was thereafter determined using Ki67 marker in NaHS or vehicle-treated cells after 24hrs. Slight but significant increases in MFI were observed in both lin^{neg} and LSK fraction of NaHS treated samples. NaHS induced H_2S release also resulted in higher percentage of LSK cells undergoing proliferation in contrast to vehicle-treated cells (Figure 3(c,d)). For further validation, in-vitro cell cycle status was analyzed after 6 and 24 h of NaHS or
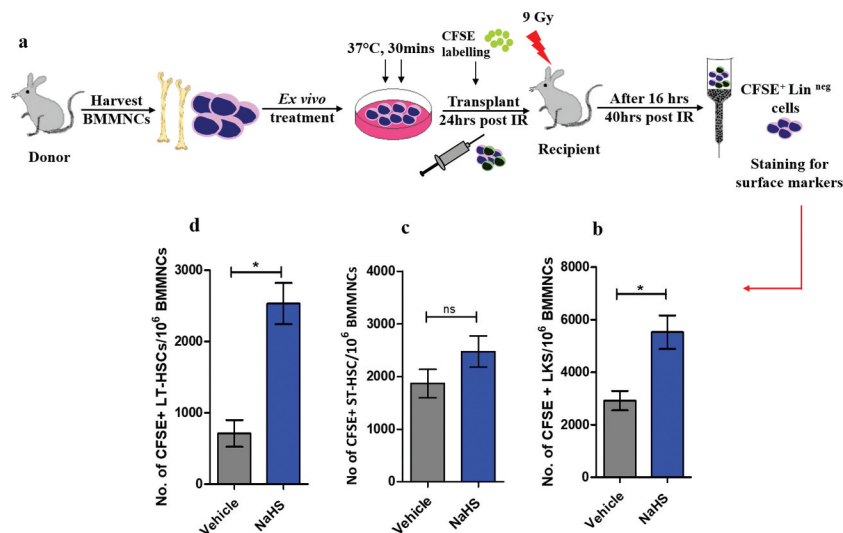
Figure 2. H₂S enhances the homing potential of HSPCs. (a) Graphical representation of experimental setup for evaluating homing of different subsets of HSPCs. 3×10^6 murine BMMNCs were treated with vehicle/NaHS, labeled with CFSE dye, washed and transplanted into lethally irradiated host mice. After 16 hrs, the host mice were sacrificed, BMMNCs isolated, lineage depleted and stained with surface markers and subsequently analyzed through flow cytometry. (b) This panel shows an increase in the homed CFSE⁺ LSK cells after NaHS treatment (n = 4 mice/group). (c) LSK population was analyzed further by staining with CD34 surface marker and CFSE⁺ LSK cells which were CD34⁺ (ST-HSCs) did not show a significant increase in the homed cells after treatment whereas, (d) a significant increase in the number of CD34⁻ (LT-HSCs) homed events were observed after NaHS treatment. Data are expressed as mean ± SEM for n = 4 mice, each assayed individually.
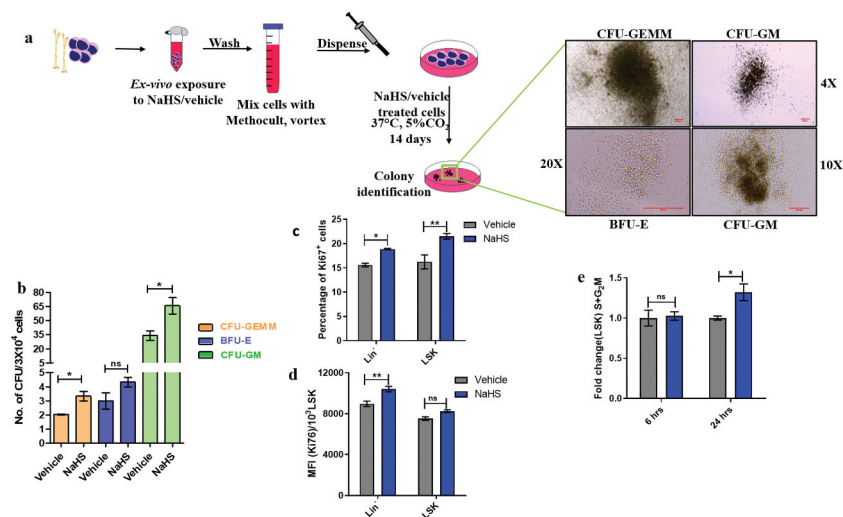

Figure 3. H₂S enhances proliferation of HSPCs and differentiation of BMMNCs in-vitro. (a) BMMNCs were pulsed with NaHS/vehicle, washed and cultured in Methocult (3X10⁴/plate) for 14 days in a CO_2 incubator at 37°C. On the 14th day, the colonies were identified as shown and scored as (b) mean ± SEM number of CFUs/3X10⁴ cells. Treated cells displayed a significant increase in the CFU-GM and CFU-GEMM. The comparisons were made using student's t-test. (n = 3, each assayed individually). (c) BMMNCs were treated with NaHS/vehicle, washed and plated in α-MEM+10% HI-FBS for 24 h. Thereafter, the cells were sorted, stained, fixed and permeabilized. Finally, the cells were stained with cell proliferation marker and the proportion of Ki67⁺ linᵐᵉᵍ and LSK cells were analyzed through flow cytometry. (d) The mean fluorescence intensity for Ki67 was also noted. Data are expressed as mean ± SEM and analyzed through two-way ANOVA. (e) Similarly, the treated cells were incubated for 6 and 24 h, thereafter sorted stained and fixed and the proportion of LSK population in cell cycle was quantified using 7-AAD viability dye through flow cytometry and represented as fold change in the S+ G₂M phase after NaHS exposure. Data are expressed as mean ± SEM and analyzed through two-way ANOVA. (n = 3,4 biological replicates, ns = non-significant *p ≤ 0.05, **p ≤ 0.01 and ***p ≤ 0.001).

vehicle-pulse exposure to cells. There was no significant change in the cycling status of LSK at 6 h but after 24 h a significant increase in the fold change was observed in the S+ G₂M phase of treated LSK, i.e., a greater proportion of NaHS exposed LSK cells were in S+ G₂M phase as compared to vehicle-treated cells (Figure 3(e)). Thus,

after pulse exposure to NaHS LSK cells were observed to be cycling at a higher frequency than vehicle control cells.

H₂S modulates intracellular calcium level and mitochondrial activity

Quiescent HSCs exhibit low membrane potential along with low levels of calcium and rely on glycolysis, not on mitochondria for energy. Thus, influx of calcium inside mitochondria drives the stem cells from low mitochondrial membrane potential ($\Delta\Psi_m$) state to high $\Delta\Psi_m$ state, thereby activating mitochondria and subsequently pushing HSCs to enter into division [23,35,36]. It was previously reported that H₂S plays a key role in the maintenance of bone homeostasis, BMMSC self-renewal and differentiation, mediated through increased intracellular calcium [16]. Since, NaHS treated cells displayed enhanced cell proliferation, the next step was to examine the intracellular calcium changes in NaHS or vehicle-treated HSPCs using Fluo-3 AM (calcium-binding dye) staining. A significant increase (1.41-fold) in intracellular calcium was observed in NaHS treated cells (in PBS for 30 min) in the presence of external calcium (1 mM CaCl₂ in PBS) as compared to vehicle control, demonstrating that H₂S enhances the influx of extracellular calcium across the plasma membrane and this calcium intake was attenuated by Nifedipine (L-type calcium channel blocker) (Figure 4(a)) [37]. As all other studies were performed in IMDM or α-MEM media with pre-added calcium, the next step was to examine the changes in intracellular calcium levels in NaHS or vehicle-treated cells in phenol red-free media and the results obtained reveal 1.38-fold elevation in intracellular calcium in LSK cells upon NaHS treatment which was inhibited by nifedipine (Figure 4(b)). Apart from this, when the study was carried out in calcium-free medium (PBS Ca²⁺ Mg²⁺ free), NaHS treated cells still showed 1.29-fold increase in MFI upon calcium binding and this data suggests that NaHS also mediates the release of calcium from intracellular stores along with influx across plasma membrane (Figure 4(c)). Since there are reports demonstrating the role of calcium in CXCR4 expression, in this study, the effect of NaHS mediated increase in calcium, on CXCR4 mRNA expression was also evaluated in the presence and absence of intracellular calcium chelator BAPTA-AM. NaHS induced increase in CXCR4 expression was found to be significantly reduced in the presence of BAPTA-AM, thus indicating the role of calcium in enhancing H₂S mediated CXCR4 expression (Figure 4(d)).

Furthermore, to investigate the activation of calcium mitochondrial pathway, changes in mitochondrial activity were determined by quantifying mitochondrial mass, mitochondrial superoxide and $\Delta\Psi_m$ in NaHS or vehicle-treated cells at 1,6 and 24 h. When compared to the immediate control (0 h), significant increases in all three parameters were observed at different time points, in NaHS treated LSK population. At 1 h time point, there was no significant change in $\Delta\Psi_m$ between treated and untreated samples. $\Delta\Psi_m$ slightly but significantly increased in NaHS treated sample after 6 h and finally elevated to 1.4-fold at 24 h time point (Figure 4(e)). Whereas, mitochondrial mass of treated cells increased to 1.42-fold (when compared to the vehicle control) within 1 h, followed by a slight drop in the fold change (1.17-fold), although still significantly higher than the vehicle control after 6 h which returned to an almost similar level as that of the control after 24 h (Figure 4(f)). No significant change in superoxide level was observed at 1 and 6 h in treated cells but after 24 h superoxide rose to a significant level in treated LSK population with a 1.25-fold increase when compared to the vehicle control (Figure 4(g)).

Effect of H₂S on cell viability and apoptosis

H₂S is a poisonous gas, which can be deleterious to mammalian cells [38]. In order to assess the overall cell health and a safe dose, HEK cells were treated with NaHS for 24 h ranging from 50 μM to 1 mM and cell viability was determined using MTT assay. As shown in the figure, cells treated with 300 μM of NaHS displayed similar reduction of MTT when compared to the vehicle-treated cells. Furthermore, increasing concentration of NaHS did not have any significant effect on cell viability for the given time duration, thus demonstrating that desired concentration of NaHS has no observed toxic effects on healthy HEK cells (Figure 5(e)). In order to further investigate the effect of NaHS treatment, apoptosis in LSK population was analyzed after 24 h of treatment at 300 μM of NaHS. No significant early (Annexin V⁺, 7-AAD⁻) and late apoptosis (Annexin V⁺, 7-AAD⁺) was observed after treatment. Additionally, the treatment did not induce any cell death as indicated by the percentage of 7-AAD⁺ cell population (Figure 5(b–d)).

NaHS enhances the repopulating potential of HSCs

After achieving significant homing of transplanted cells, it was determined whether the treated cells can repopulate significantly when compared to the control. Changes in various hematopoietic parameters in peripheral blood were evaluated by using automated hematology analyzer to determine whether the H₂S treatment can ameliorate
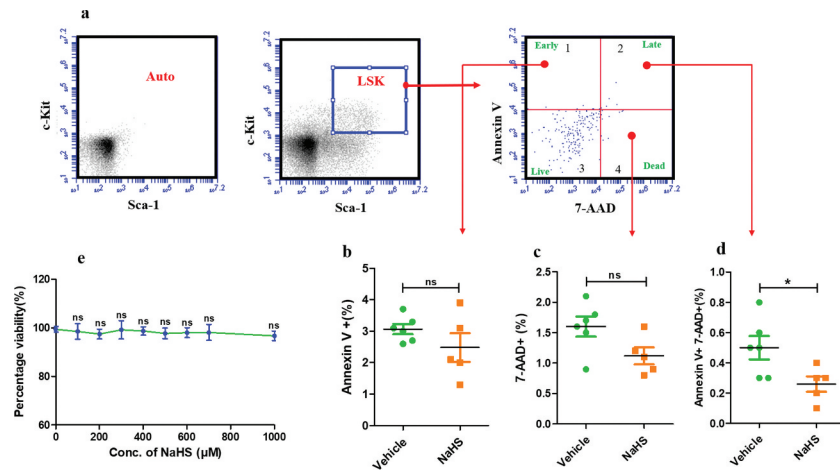
Figure 4. Modulation of intracellular calcium and mitochondrial activity by H2S and the effect of NaHS mediated Calcium influx on CXCR4 expression. (a) Graphs depict the MFI of Fluo-3AM indicative of intracellular calcium measured in LSK cells. The experiment was done in PBS with or without $CaCl_2$ in the presence or absence of NaHS and Nifedipine (NF, L-type calcium channel blocker). (b) intracellular calcium levels before and after NaHS/NF treatment in LSK population when the cells were incubated in the IMDM media (containing pre-added $CaCl_2$, phenol red free) (c) the effect of H_2S on intracellular calcium levels in HEK cell line in the presence and absence of $CaCl_2$ indicating the effect of H2S not only in LSK fraction of mice but in the other cells also. (d) Fold change in CXCR4 expression in BMMNCs in vehicle/NaHS/BAPTA-AM treated cells demonstrating the role of calcium in NaHS mediated increase in CXCR4 expression. (e) Line graphs indicating the gradual rise in MFI of Rh123, a mitochondrial membrane potential dye after 6,12 and 24 h in NaHS/vehicle treated cells (LSK fraction). (f) mitochondrial mass in LSK proportion using Mitotraker green (g) Mitochondrial superoxide level in vehicle/NaHS treated LSK population using Mitosox red indicator at 3 different time points. (h) summary of the proposed mechanism. Data are expressed as fold change in MFI (wrt control) for n = 3 and all the statistical comparisons were done using One-way ANOVA and Bonferroni posttest.

radiation-induced leukocytopenia, erythropenia, and thrombocytopenia (Figure 6(a)). It is already reported that radiation leads to a significant loss of blood cells and in this study, it was observed that transplantation of treated cells resulted in a slight increase in all the hematopoietic parameters. The increase in the number of total WBCs (Figure 6(b)) and granulocytes (Figure 6(d)) were found to be significant in the case of treatment whereas other parameters like the number of lymphocytes (Figure 6(c)), RBCs (Figure 6(e)), platelets (Figure 6(g)), amount of

hemoglobin (Figure 6(f)) and the percentage hematocrit (HCT) (Figure 6(h)) displayed only a slight increase and were not significant when compared to the control after 21 days post-irradiation.

Discussion

Bone marrow transplantation has become an indispensable strategy for managing hematopoietic malignancies such as hematopoietic form of acute radiation

Figure 5. Effect of H$_2$S treatment on apoptosis in LSK population and HEK cell viability. (a) Representative gating strategy followed for detecting apoptosis in LSK population after 24 hrs in NaHS/vehicle treated cells using AnnexinV-FITC and 7-AAD. (b) The proportion of LSK population in the quadrant 1 i.e. Annexin V$^+$, indicating early apoptosis which was non-significant after treatment. (c) The percentage of 7-AAD positive cells (quadrant 4) i.e. dead cells, non-significant after treatment. (d) The proportion of cells that are both positive (AnnexinV$^+$7-AAD$^+$), demonstrating late apoptosis 24 h after treatment (vehicle/NaHS). Data are expressed as mean ± SEM for n = 4 and the comparisons were done using Student's t-test. (e) Toxicity assessment of NaHS on HEK cells using MTT assay. HEK cells were treated with vehicle/NaHS (100–1000 μM) for 24 h, washed and incubated with MTT for 4 h. Thereafter, the formazan crystals were dissolved in DMSO and the absorbance was read and the data are expressed as mean ± SEM percentage viability for n = 6. The data was analyzed using one-way ANOVA and Bonferroni posttest.
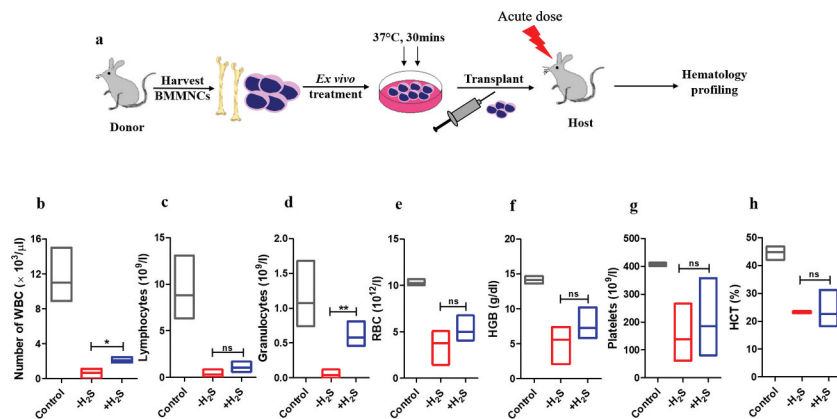

Figure 6. Hematology profiling of irradiated recipient mice after transplantation. Whole Bone marrow cells were isolated in sterile conditions, RBC lysis was done, washed and resuspended in sterile 1X PBS. BMMNCs were enumerated, NaHS/vehicle treated and transplanted into acutely irradiated recipient mice after 24 h. Changes in the number of (a) total white blood cells (WBC) (b) lymphocytes (c) granulocytes (d) RBCs (e) hemoglobin (f) hematocrit percentage and (g) platelets were measured on 21st post irradiation day. Each value is a mean ± SEM (n = 3–4 animals/group) and the comparisons are done using unpaired t-test.

syndrome. Several researchers have proposed ex-vivo manipulation of HSCs to enhance the homing and engraftment efficiency in order to achieve successful transplantation since limited number of HSCs is a major constraint to its use. Despite its merit, the strategies employed are expensive and may not be feasible for all. The cost of HSC transplant in itself is high and on top of it, utilizing strategies that employ expensive molecules would be an extra burden. So, in this study, NaHS have been employed as a donor of H$_2$S which displays a potential to enhance the homing of

the HSPCs and is also cost-effective at the same time. It is well documented that H$_2$S as an endogenous gasotransmitter is involved in the maintenance of Bone marrow mesenchymal stem cells and bone homeostasis [16]. It is already established that H$_2$S plays a role in promoting HSPC differentiation and providing protection against fatal myelosuppression by stimulating megakaryocytopoiesis [39]. It is a known regulator of calcium and mediates calcium influx through various calcium channels including L-type, T-type and also via sulfhydration of TRP channels [16,17]. There are

evidence that NaHS as an H_2S donor acts as a neuromodulator by increasing calcium influx from extracellular environment as well as calcium mobilization from intracellular stores, thus maintaining calcium homeostasis in neurons [36]. Additionally, H_2S is reported to stimulate angiogenesis, cell proliferation, migration in endothelial cells in culture as well as a known promoter of angiogenesis in mice in-vivo along with proliferative and anti-apoptotic effects on hepatoma cells [40–42].

Through this study, the effect of ex-vivo exposure of NaHS on hematopoietic stem and progenitor cells has been demonstrated. Evaluation of mRNA expression revealed a significant increase in NaHS exposed BMMNCs, suggesting its potential in homing. Trans-well migration assay displayed an enhanced CXCR4 migratory response of HSPCs toward SDF-1α in vitro. A significant proportion of LSK population migrated towards SDF-1α when compared with the control. Transplantation of NaHS exposed BMMNCs in lethally irradiated mice resulted in a significant increase in the proportion of homed LSK cells in the recipient's bone marrow niche. Furthermore, in-vitro studies revealed that NaHS short-term exposure significantly elevated cell proliferation marker, Ki67 after 24 h. Cell cycle analysis showed that NaHS treatment resulted in more percentage of cycling LSK cells, i.e., a higher proportion of cells were in S+ G_2M phase, 24 h after the NaHS exposure. This data is in concordance with the previous reports demonstrating the proliferation and angiogenic potential of H_2S in different cell types [40,41]. However, NaHS exposure also leads to enhanced differentiation of BMMNCs as evident through colony-forming assay which displayed a significant increase in colonies CFU-GM and CFU-GEMM. Although H_2S is poisonous gas, but NaHS induced H_2S release had no significant effect on the viability of HEK cells and also no significant apoptosis was observed in NaHS treated LSK cells, 24 h after treatment.

Furthermore, the modulation of mitochondrial activity and increased intracellular calcium levels by NaHS was evaluated as a possible mechanism for enhancing the cell proliferation, survival, and homing of HSPCs. Based on the previous reports that calcium-mitochondrial axis is responsible for driving quiescent HSCs into division and H_2S is responsible for mediating the influx of calcium through various calcium channels leading to the rise in intracellular calcium, the role of H_2S on mitochondrial activity and calcium levels in LSK population was further investigated [16,17,23]. NaHS treatment resulted in a significant rise in the intracellular calcium in LSK and Lin^{neg} population, both in the presence and absence of calcium, indicating that NaHS induces calcium release from the intracellular calcium stores as well as influx from the extracellular environment. NaHS treated LSK population showed a significant increase in MMP after 6 h which further increased after 24 h. Pulse exposure also resulted in a significant elevation in mitochondrial mass at 1h and 6 h which returned to normal after 24 h. There was no significant increase in superoxide generation after 1 and 6 h but after 24 h superoxide level significantly increased in the NaHS treated LSK cells. The above data suggests that along with the changes in the calcium level H_2S is also capable of modulating mitochondrial activity which might be one of the reasons, contributing towards the enhanced cell proliferation.

There are previous reports linking the role of extracellular calcium to increased CXCR4 expression indicating the importance of calcium signaling in CXCR4 expression [20]. The effect of H_2S induced calcium increase on the CXCR4 expression in BMMNCs was therefore examined. CXCR4 mRNA expression was significantly reduced in the presence of BAPTA AM when compared to NaHS treated group indicating the role of calcium in enhancing CXCR4 expression. These results might suggest that the elevation of CXCR4 in NaHS treated cells can be attributed to the increased intracellular calcium levels which is reduced by the intracellular calcium chelator BAPTA AM. Based on this study, it can be hypothesized that H_2S induced increase in calcium might be the possible mechanism through which it mediates mitochondrial activity, cell proliferation, CXCR4 expression, and subsequently homing of HSPCs to their niche.

In conclusion, this study proposes that short term ex-vivo exposure of BMMNCs to H_2S is a viable and cost-effective strategy and that the increased homing of the available number of HSCs can alleviate the need of ex-vivo expansion. The exact mechanism of action through which H_2S enhances CXCR4 expression and mediates intracellular calcium levels still needs to be assessed. Detailed engraftment studies including long-term and short-term repopulating potential of NaHS treated cells needs to be further evaluated and hematology profiling post-21-days could provide some conclusive answers which might open a gateway for its future use. Further NaHS treatment must be validated on umbilical cord blood (UCB) cells and the effect of this treatment on CXCR4 expression and homing using UCB cells still remains unanswered which is essential for improving its clinical utility.

Statistical analysis

All the data values are represented as mean ± standard error of mean (SEM) and statistical analysis was done in GraphPad Prism Software (v5.0, La Jolla, CA, USA).

Differences between control and treated were calculated by one-way ANOVA, two-way ANOVA followed by Bonferroni post-test for multiple comparison and Student's t-test for single comparison. Significance level is denoted as $*p \leq 0.05$, $**p \leq 0.01$, $***p \leq 0.001$ and ns, non-significant

Authors contribution

AK and IPK conceived the presented idea. AK performed all the experiments and the data were analysed by AK, IPK, IN, and RC. All authors discussed the results and contributed to the final manuscript.

Disclosure statement

No potential conflict of interest was reported by the authors.

Ethics approval

Animal handling and all animal experiments followed protocols approved by the Committee on the Ethics of Animal Experiments, Institute of Nuclear Medicine and Allied Sciences (INMAS), Defence Research and Development Organization (DRDO).

Informed consent

Not applicable since the manuscript does not contain any patient data.

ORCID

Anoushka Khanna http://orcid.org/0000-0001-6601-8762
Prem Kumar Indraganti http://orcid.org/0000-0003-3321-880X

References

[1] Ballen KK, Gluckman E, Broxmeyer HE. Umbilical cord blood transplantation: the first 25 years and beyond. Blood. 2013;122(4):491–498.

[2] Ratajczak MZ, Suszynska M. Emerging strategies to enhance homing and engraftment of hematopoietic stem cells. Stem Cell Rev Rep. 2016;12(1):121–128.

[3] Liu X, Wang J, Ji X, et al. Preconditioning of bone marrow mesenchymal stem cells by prolyl hydroxylase inhibition enhances cell survival and angiogenesis in vitro and after transplantation into the ischemic heart of rats. Sten Cell Res Ther. 2014;5(111):1–12.

[4] Hu X, Yu SP, Fraser JL, et al. Transplantation of hypoxia-preconditioned mesenchymal stem cells improves infarcted heart function via enhanced survival of implanted cells and angiogenesis. Cardiopulm Support Physiol. 2008;135(4):799–808.

[5] Mantel CR, O'Leary HA, Chitteti BR, et al. Enhancing hematopoietic stem cell transplantation efficacy by mitigating oxygen shock. Cell. 2015;161(7):1553–1565.

[6] Morrison SJ, Scadden DT. the bone marrow niche for HSCs. Nature. 2014;505(7483):327–334.

[7] Bradley TR, Hodgson GS, Rosendaal M. The effect of oxygen tension on haemopoietic and fibroblast cell proliferation in vitro. J Cell Physiol. 1978;97(3):517–522.

[8] Lam BS, Cunningham C, Adams GB. Pharmacologic modulation of the calcium-sensing receptor enhances hematopoietic stem cell lodgment in the adult bone marrow. Blood. 2019;117(4):1167–1175.

[9] House MG, Kohlmeier L, Chattopadhyay N, et al. Expression of an extracellular calcium - sensing receptor in human and mouse bone marrow cells. J Bone Miner Res. 2009;12(12):1–24.

[10] Hoggatt J, Singh P, Sampath J, et al. Prostaglandin E2 enhances hematopoietic stem cell homing, survival, and proliferation. Blood. 2009;113(22):5444–5455.

[11] Yaegaki K, Sci BJ, Res T, et al. Role of hydrogen sulfide, biologically-active compound, during cell de-differentiation and differentiation processes. Biomed J Sci Tech Res. 2018;3(4):1–13.

[12] Shefa U, Kim M, Jeong NY, et al. Antioxidant and cell-signaling functions of hydrogen sulfide in the central nervous system. Oxid Med Cell Longev. 2018;2018:17.

[13] Han Y, Shang Q, Yao J, et al. Hydrogen sulfide: a gaseous signaling molecule modulates tissue homeostasis : implications in ophthalmic diseases. Cell Death Dis. 2019;10:1–12.

[14] Li L, Rose P, Moore PK. Hydrogen sulfide and cell signaling. Annu Rev Pharmacol Toxicol. 2011;51:169–187.

[15] Tang C, Li X, Du J. Hydrogen sulfide as a new endogenous gaseous transmitter in the cardiovascular system. Curr Vasc Pharmacol. 2005;4(1):17–22.

[16] Liu Y, Yang R, Liu X, et al. Article hydrogen sulfide maintains mesenchymal stem cell function and bone homeostasis via regulation of Ca 2 + channel sulfhydration. Stem Cell [Internet]. 2014;15:1–13.

[17] Moccia F, Bertoni G, Pla AF, et al. Hydrogen sulfide regulates intracellular Ca 2 + concentration in endothe- lial cells from excised rat aorta. Curr Pharm Biotechnol. 2011;12(9):1416–1426.

[18] Zhang W, Xu C, Yang G, et al. Interaction of H 2 S with calcium permeable channels and transporters. Oxid Med Cell Longev. 2014;2015:1–8.

[19] Buckler KJ. Effects of exogenous hydrogen sulphide on calcium signalling, background (TASK) K channel activity and mitochondrial function in chemoreceptor cells. Signal Cell Physiol. 2012;463(5):743–754.

[20] Wu Q, Shao H, Darwin Eton D, et al. Extracellular calcium increases CXCR4 expression on bone marrow-derived cells and enhances pro-angiogenesis therapy. J Cell Mol Med. 2009;13(9):3764–3773.

[21] Mazo IB, Massberg S, Von Andrian UH. Hematopoietic stem and progenitor cell trafficking

Hematopoietic stem cells: characteristic features. Trends Immunol. 2012;32(10):493–503.

[22] Sahin AO, Buitenhuis M. Molecular mechanisms underlying adhesion and migration of hematopoietic stem cells. Cell Adh Migr. 2012;6(1):39–48.

[23] Umemoto T, Hashimoto M, Matsumura T, et al. Ca 2 + – mitochondria axis drives cell division in hematopoietic stem cells. J Exp Med. 2018;215(8):2097–2113.

[24] Mariani M, Colombo F, Assennato SM, et al. Evaluation of an easy and affordable flow cytometer for volumetric haematopoietic stem cell counting. Blood Transfus. 2014;12(3):416–420.

[25] Osawa M, Hanada K, Hamada H. Long-term lymphohematopoietic reconstitution by a single CD34-low/negative hematopoietic stem cell. Science. 1996;273(5272):242–245.

[26] Ishida T, Suzuki S, Lai CY, et al. Pre - ttransplantation blockade of TNF - α - mediated oxygen species accumulation Pro - tects hematopoietic stem cells. Stem Cells. 2016;35(4):986–1002.

[27] Livak KJ, Schmittgen TD. Analysis of relative gene expression data using real- time quantitative PCR and the 2 method. Methods. 2001;25(4):402–408.

[28] Guo B, Huang X, Cooper S, Broxmeyer HE. Glucocorticoid hormone-induced chromatin remodeling enhances human hematopoietic stem cell homing and engraftment. Nature Medicine. 2017 Apr;23 (4):424–428.doi: 10.1038/nm.4298.

[29] Pereira C, Clarke E, Damen J. Hematopoietic colony-forming cell assays. Methods Mol Biol. 2007;407:177–208.

[30] Cancelas JA. Adhesion, migration, and homing of murine hematopoietic stem cells and progenitors. Methods Mol Biol. 2011;750:187–196.

[31] Quah BJC, Warren HS, Parish CR. Monitoring lymphocyte proliferation in vitro and in vivo with the intracellular fluorescent dye carboxyfluorescein diacetate succinimidyl ester. Nat Protoc. 2007;2(9):2049–2056.

[32] Rosenkilde MM, Gerlach LO, Jakobsen JS, et al. Molecular mechanism of AMD3100 antagonism in the CXCR4 receptor: transfer of binding site to the CXCR3 receptor. J Biol Chem. 2004;279(4):3033–3041.

[33] Yusuf RZ, Scadden DT. Homing of hematopoietic cells to the bone marrow. J Vis Exp. 2009;25:1104.

[34] Seita J, Weissman IL. Hematopoietic stem cell: self-renewal versus differentiation. Wiley Interdiscip Rev Syst Biol Med. 2010;2(6):640–653.

[35] Baldridge MT, King KY, Boles NB, et al. Quiescent hematopoietic stem cells are activated by IFN gamma in response to chronic. Nature. 2010;465 (7299):793–797.

[36] Mendelson A, Frenette SP. Hematopoietic stem cell niche maintenance during homeostasis and regeneration. Nat Med. 2014;208:833–846.

[37] Yong QC, Choo CH, Tan BH, et al. Effect of hydrogen sulfide on intracellular calcium homeostasis in neuronal cells. Neurochem Int. 2010;56(3):508–515.

[38] Jiang J, Chan A, Ali S, et al. Hydrogen sulfide — mechanisms of toxicity and development of an antidote. Sci Rep. 2016;6(20831):1–10.

[39] Liu H, Zhang A, Xu J, et al. H 2 S protects against fatal myelosuppression by promoting the generation of megakaryocytes/platelets. J Hematol Oncol. 2016;9:1–13.

[40] Szabó C, Papapetropoulos A. Hydrogen sulphide and angiogenesis : mechanisms and applications. Br J Pharmacol. 2011;164:853–865.

[41] Papapetropoulos A, Pyriochou A, Altaany Z, et al. Hydrogen sulfide is an endogenous stimulator of angiogenesis. PNAS. 2009;106(51):21972–21977.

[42] Zhen Y, Pan W, Hu F, et al. Exogenous hydrogen sulfide exerts proliferation/anti-apoptosis/angiogenesis/migration effects via amplifying the activation of NF- κ B pathway in PLC/PRF/5 hepatoma cells. Int J Oncol. 2015;46:2194–2204.